

Influence of magnetic field on the Doppler measurements of velocity field in the solar photosphere and implications for helioseismology

S. P. Rajaguru¹, R. Wachter¹ and S. S. Hasan²

¹W.W. Hansen Experimental Physics Laboratory, Stanford University, Stanford CA 94305, USA

²Indian Institute of Astrophysics, Bangalore-560036, India

Abstract. Shapes of spectral lines and their sensitivity to fluid motions are strongly altered in magnetised regions of the solar atmosphere. Sunspots and plages (bright network regions) are prime examples. Here we study the temporal behaviour of Ni I (6768 Å, used by MDI onboard SOHO) in sunspots and plages using realistic models of sunspots and network flux tubes as input to a radiative transfer code SPINOR (Frutiger et al., 2000) that models spectral line formation in magnetic fields. We examine the sunspot case based on a simple model of oscillations superposed on the Maltby model (empirical) of sunspot atmosphere. The plage regions are studied using a 2-d MHD simulation of oscillatory motions (Hasan et al., 2005) in network flux tubes. We discuss the changes that the altered line profiles would cause in the Doppler measurements of the velocity field, especially those by helioseismic imaging instrument MDI onboard SOHO.

Index Terms. Sun- helioseismology, Sun-magnetic field, Sun- oscillations, Sun- spectral lines.

1. Introduction

It is well known that the Zeeman splitting, due to strong magnetic field and the altered thermal conditions inside sunspots, change the shape and strength of magnetically sensitive spectral absorption lines drastically. These changes affect Doppler velocity measurements (Alamanni et al., 1990; Balthasar and Schmidt, 1993; Bogdan, 2000) and are expected to cause systematic errors; especially, when they are done from images (of polarization states) at a few wavelength locations across a line (Wachter et al., 2006), which is typical of helioseismic instruments such as MDI onboard SOHO. Here we study the temporal behaviour of Ni I (6768 Å) line in response to a simple simulated velocity oscillation signal in a sunspot atmosphere as well as to a 2-d MHD simulated wavefield in a flux sheet (Hasan et al., 2005). We model the spectral line formation in magnetic fields using the STOPRO routines (Solanki, 1987) that form part of a spectral inversion code “SPINOR”(Frutiger et al., 2000). This code solves the Unno-Rachkovsky radiative transfer equations assuming LTE (Local Thermodynamic Equilibrium) conditions. We compare the appropriately weighted (in height) input velocity field, by use of calculated spectral response functions (RF’s), with those returned by a helioseismic Doppler measurement algorithm used by the MDI instrument onboard SOHO. The MDI Doppler algorithm uses images (or filtergrams) scanned over 5 positions along the spectral line in polarized states (Stokes profiles) and combines them to get the line of sight velocity and magnetic fields (Scherrer et al., 1995).

2. Synthesis of Ni I line in magnetized atmospheres

We synthesize the Stokes profiles of the Ni I (6768 Å) line at each time step of simulated oscillations in all the atmospheric quantities (that include pressure p , temperature T , density ρ , magnetic field \mathbf{B} , line of sight velocity (LOS) v , opacity κ , angle γ between \mathbf{B} and LOS, and azimuthal angle χ of \mathbf{B}) using the “STOPRO” routines that are part of the code “SPINOR” (Frutiger et al., 2000). The construction of atmospheric quantities with simulated oscillation field is done as discussed in the following sub-section.

2.1 Sunspot model with imposed oscillations

We use the Maltby M sunspot model (Maltby et al., 1986) for the run of atmospheric parameters as a function of height z . We calculate the height variation of magnetic field strength in the Maltby model by prescribing a value for Wilson depression and using the horizontal pressure balance with the quiet-sun atmosphere, which is also taken from the Maltby et al. (1986) models. We control the value of the magnetic field at the observable height using the Wilson depression as a free parameter. We calculate a spectrum of solar oscillations in the quiet-sun model at angular degree $l=200$ by solving the nonadiabatic boundary value problem (Unno et al., 1989), which accounts for the radiative energy flux in the diffusion approximation (see Wachter, 2004 for a description). We excite the oscillations using a radial force source located 100 km beneath the base of the photosphere. The time series corresponding to this spectrum is then calculated by an inverse Fourier transform resulting in a 128 minute series with one minute sampling time. We then add the oscillation signals in the atmospheric quantities to the Maltby M sunspot model; this addition does not model the oscillations that a

sunspot can support, but serves our purpose of examining the influence of sunspot structure on the spectral line shapes and consequently on the Doppler signatures of the imposed oscillations. However, the present study does not include a consistent modeling of waves in sunspots and their effects on spectral line formation but just aims to study the influence of mean sunspot structure on Doppler measurements.

2.2 MHD simulation of waves in a magnetic flux sheet

We use a 2-d MHD simulation of waves in a network flux element modeled as a magnetic flux sheet with a nonpotential field structure with a typical horizontal size of about 150 km at the base of the photosphere (Hasan *et al.*, 2005). The waves are generated by a periodic excitation of waves due to a transverse driving of the lower boundary located at the photosphere, with a period of 24 s and with an amplitude of 750 m/s. We refer to Hasan *et al.* (2005) for a detailed description of the simulation and the physics of generated waves. Fig.1 shows the magnetic field structure of the flux sheet and Fig. 2 shows a snapshot of the line of sight velocity (vertical) at the last instant (192 s) of the simulation over the central portion of the flux sheet.

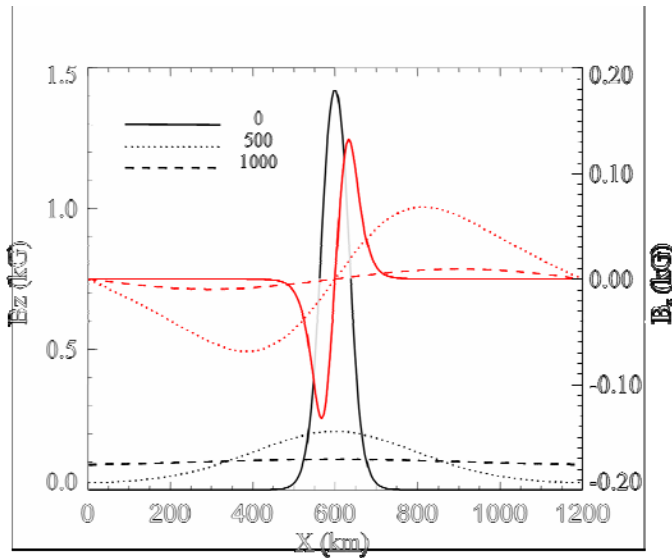


Fig. 1. Variation of B_z with horizontal distance (from the left edge of the computational domain) at the following heights: $z=0$ (black solid line), 500 km (black dotted line) and 1000 km (black dashed line). The corresponding red curves denote B_x measured with respect to the values given on the right scale.

The simulation domain starts from the photospheric height. Since the spectral line formation in the solar atmosphere includes contributions from layers up to a certain depth below the photosphere, we append a suitably constructed sub-photospheric layer for the flux sheet. The horizontal structure is determined by balancing the total (magnetic + gas) pressure and by conserving the magnetic flux from the photosphere to deeper layers. The simulation runs for a total time extent of 192 s in 22 time steps.

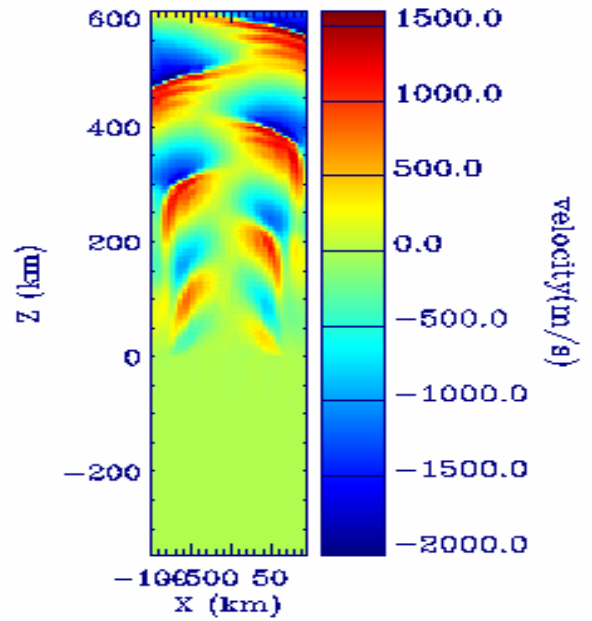


Fig. 2. A snapshot of LOS velocity v at the last time instant of 2-d MHD simulation over the horizontal 200 km central portion of the flux sheet.

3. Simulating the MDI Doppler measurements

The MDI consists of two tunable Michelson interferometers and a Lyot filter, which realize successively five narrow-banded filters $F_0 \dots F_4$ with a separation of 75 mÅ. These filters cover the observed Doppler shift of the Ni I absorption line. The filter profiles and a sample observation of the absorption line are displayed in Fig. 3. From the following two functions $\alpha_>$ and $\alpha_<$ given by,

$$\begin{aligned} \alpha_> &= ((F_1 - F_3) + (F_2 - F_4)) / (F_1 - F_3) \\ \alpha_< &= ((F_1 - F_3) + (F_2 - F_4)) / (F_4 - F_2) \end{aligned} \quad (1)$$

($\alpha_> = \alpha$ for a positive numerator, $\alpha = \alpha_<$ for a negative numerator), the line of sight velocity is obtained by a nearly linear calibration function. This MDI Doppler velocity is defined to be positive for velocities away from the observer.

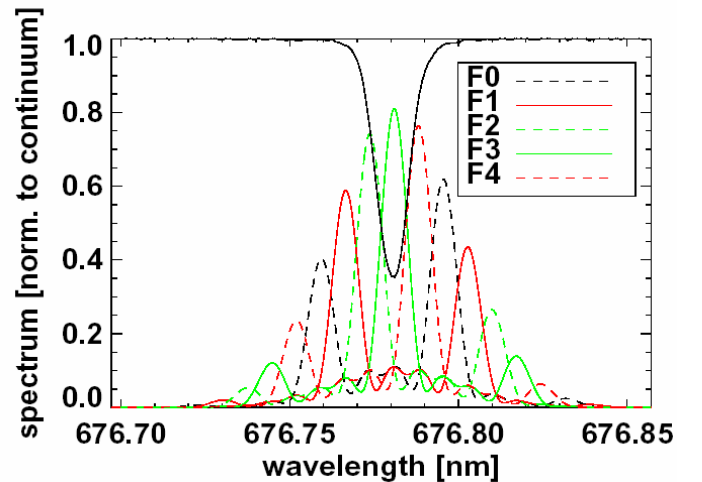


Fig. 3. MDI filter profiles over a sample profile of Ni I (6768 Å) absorption line (observed at NSO/Kitt Peak FTS).

The MDI measures the LOS velocity in two different modes: in one of the linear polarization states, Stokes I+Q, and in the two circular polarization states, Stokes I+V and I-V, i.e., by measuring the filtergram signals in these polarization states. The LOS velocity from the two circular polarization signals, left (LCP) and right (RCP), are just the average of the two velocity signals and the LOS magnetic field B is the difference with a certain normalization:

$$\begin{aligned} V_{\text{LOS}} &= (V_{\text{LCP}} + V_{\text{RCP}})/2 \\ B_{\text{LOS}} &= (V_{\text{LCP}} - V_{\text{RCP}})/2.84 \end{aligned} \quad (2)$$

4. Results

4.1 Sunspot with imposed oscillations

We show in Fig. 4 sample profiles synthesized in a Maltby sunspot model with a photospheric LOS field strength of 2955G, which corresponds to a Wilson depression of 350 km in our calculation. We note that, in our line profile synthesis, we have not attempted to include any effects of instrument on the profiles nor taken account of noise sources of any origin. Hence, the results that we present are aimed at modeling the influence of physics that we put in, which controls the line shape changes.

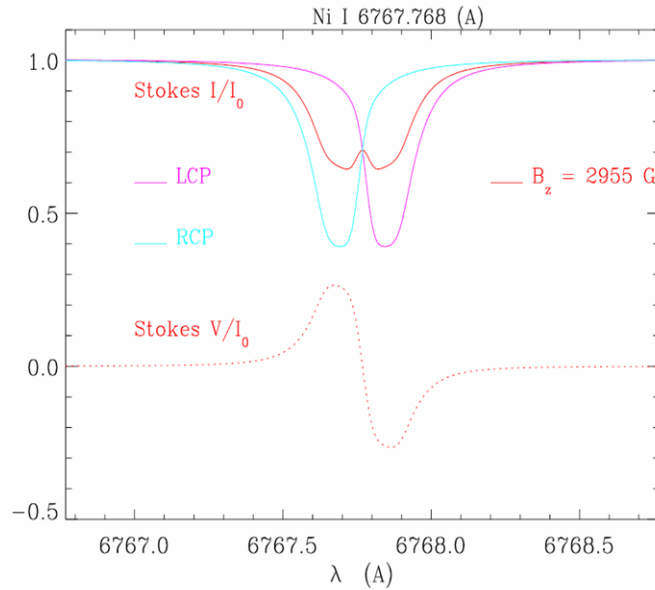


Fig. 4. Synthesized Stokes profiles of Ni I (6768 Å) line in the Maltby M model atmosphere of sunspot with a LOS photospheric field strength of 2955 G.

We find that, for the case of pure oscillations superposed on the Maltby sunspot model, the MDI circular polarization measurements, as given by Eqns. (2), very accurately measure the Doppler shifts of the Ni I line over a wide range of inclination angle γ of \mathbf{B} . However, measurements in linear polarization state (Stokes I + Q) performed by MDI (which is the mode of observation in the full-disk resolution imaging by MDI) impair the phase evolution of the Doppler signals very much leading to large phase shifts between the input and

output signals when the field lines are aligned to the LOS ($\gamma = 0$). However, such phase shifts go down sharply as γ increases. The results are summarized in Fig. 5 and 6. These results show that Doppler measurement algorithms such as that of MDI, and in general measurements based on Fourier phase shifts in line profiles, lead to substantially impaired phase evolution of oscillation signals when the line profiles have split shapes.

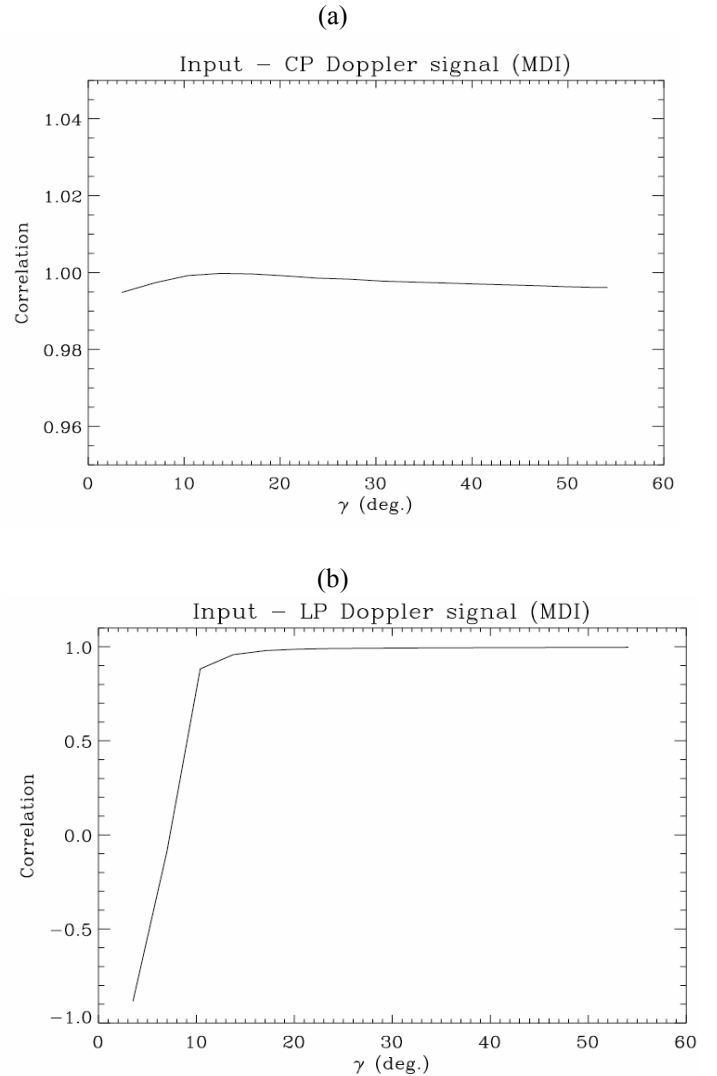


Fig. 5. Input vs Output (by MDI) correlations as a function of inclination angle γ of \mathbf{B} to the LOS. Panel (a) is measurements based on the left and right circularly polarized components of the line profile, and panel (b) is measurements from linearly polarized component I+Q.

4.2 MHD simulated waves and Doppler measurements

The 2-d MHD simulations of waves in a flux sheet described in section 2.2 are used to synthesize the Ni I line and the measurements of Doppler shifts are carried out simulating the MDI instrument as in the previous Section. We additionally calculate the Doppler velocities using the center of gravity method (COG) as well (Uitenbroek, 2003). The height dependent input velocities are averaged over height by use of

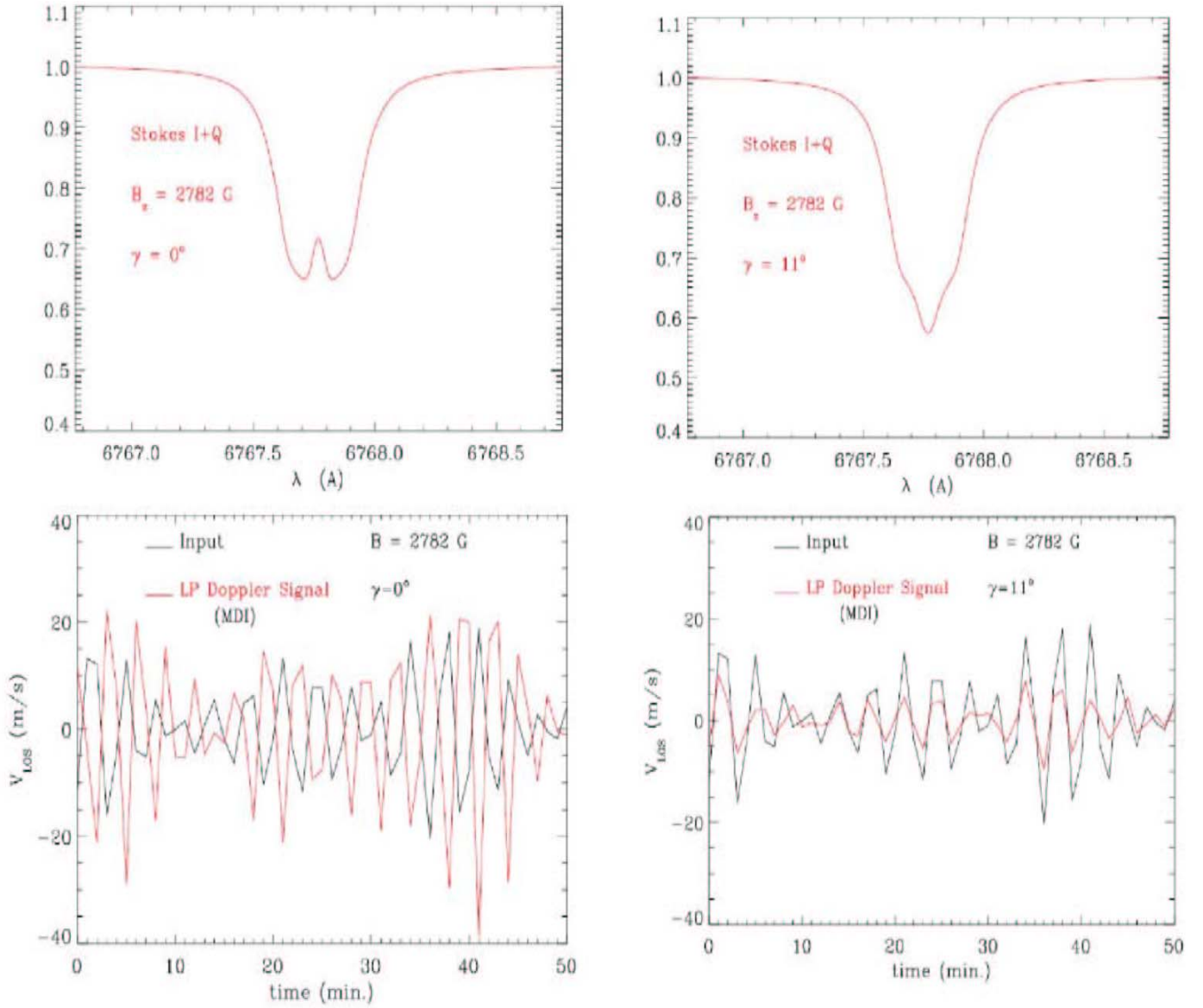


Fig. 6. Linear polarization (I+Q) line profiles with two different γ (as marked in the panels) (top row), with the corresponding comparison of input vs output oscillation signals (bottom row).

wavelength integrated (over the range covering the absorption line) velocity response functions (RF's), that are calculated by the STOPRO routines while synthesizing the line (Frutiger 2000). These RF's, thereby, consistently take into account the changes in the line formation heights within the magnetized atmosphere. An example of the weight functions (which are wavelength integrated RF's) are shown in Fig. 7. The changes in the formation heights of the line are clearly evident from the height variation of the response functions, which are shown for LOS in a weak field region and at the center of the flux tube (we use the terms 'flux tube' and 'flux sheet' interchangeably).

Figs. 8 and 9 show the comparison of input (weighted by RF's shown in Fig. 7) from the MHD simulations and those returned by the three different Doppler measurement

procedures, viz. MDI circular and linear polarization measurements, and the COG method. From the results in these figures, we see that the best measurements are achieved using circularly polarized components of line profiles. The reduction in correlation between the input and output signals, as seen in Fig. 9, are mainly at horizontal locations where the vertical gradients and amplitudes of the signals are the largest. We, however, are not able to isolate a single dominant quantity that is responsible for the reduction in the input-vs-output correlations. The sharp fall in the correlations close to the sheath axis (at $x=0$ km), in Fig. 9, for the MDI linear polarization and COG methods are likely to be a consequence of sharper vertical gradients in the various atmospheric quantities at those locations.

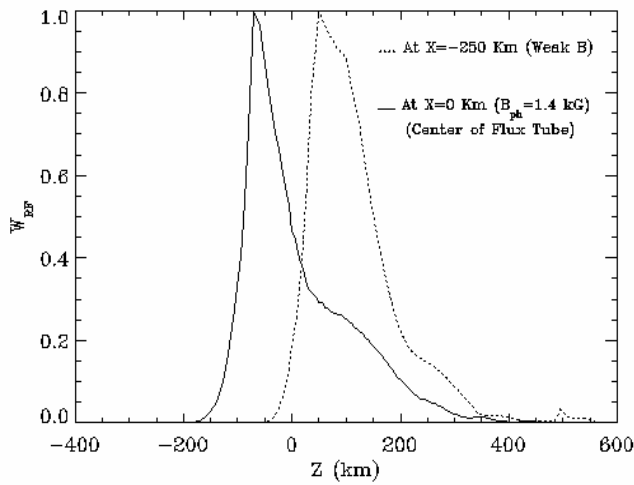


Fig. 7. Weight functions, WRF, which are wavelength integrated velocity response functions (RF's), as a function of height in the atmosphere for two different horizontal positions across the flux sheet.

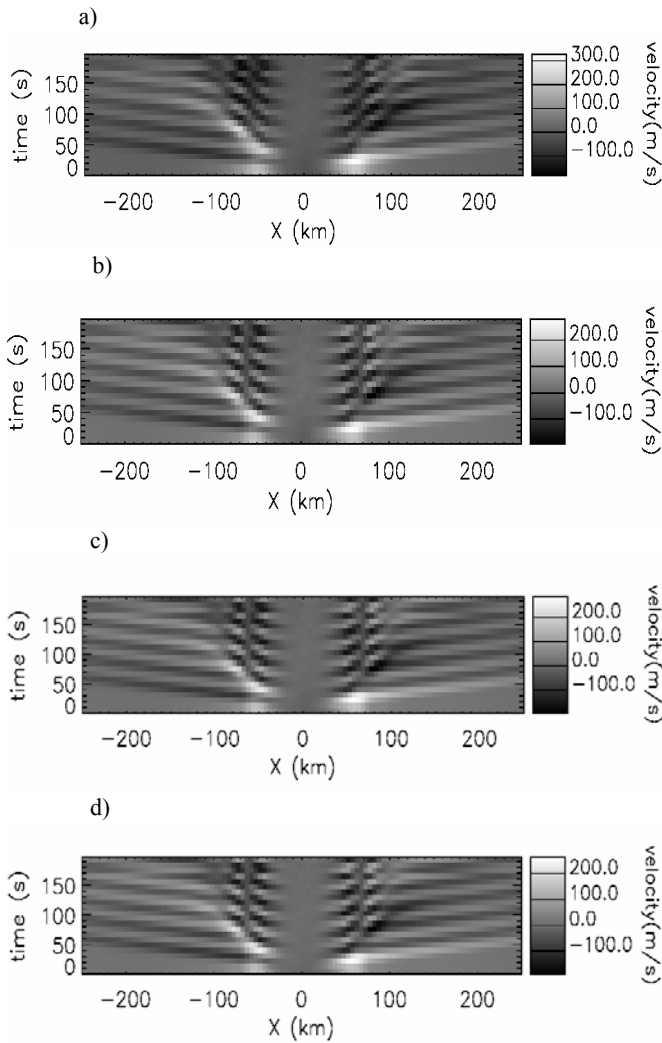


Fig. 8. The velocity signals across (in the x-direction) the flux sheet as a function of time: a) the input field weighted in height according to the velocity RF's (examples shown in Fig. 7), and in b), c) and d) are outputs returned by, respectively, the MDI circular polarization, linear polarization and the COG methods.

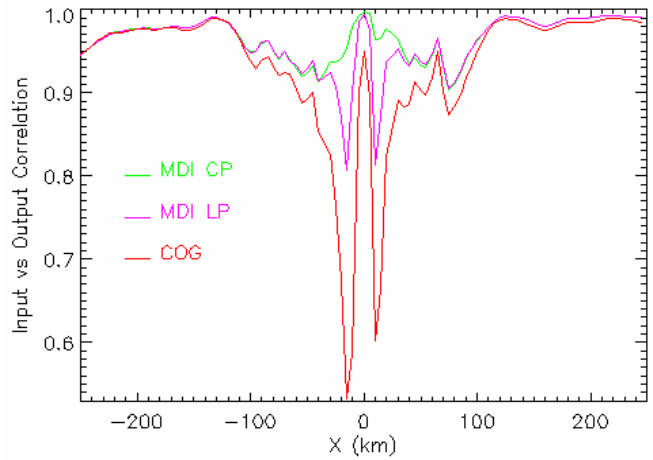


Fig. 9. Correlations between the input (Fig. 8a) and the outputs returned by the three Doppler measurement algorithms: the different color lines correspond to the different methods as marked inside the figure panel.

5. Discussion

The results presented in the previous section, in a rather qualitative manner, show that split line profiles, such as that may arise due to Zeeman effect in strong magnetic field regions, may cause spurious phase shifts in the measured Doppler velocity signals. In addition, it is seen that large amplitude velocities with vertical steep gradients such as those arising in higher atmospheric layers - low to mid-chromospheric regions - of a magnetized region, can further contribute to impaired retrieval of phase as well as amplitudes of Doppler signals from spectral lines.

Use of Doppler velocity measurements made within strongly magnetized regions such as sunspots require corrections before they can be used for studies that exploit the phase and amplitude information of waves. Such information are the main ingredients in local helioseismology, and hence these studies are highly likely to suffer from systematics that may lead to wrong 'physical' signals in the inferences of sub-surface structure and dynamics.

A quantitative, systematic and detailed study of the various effects involved in the thermo-mechanical evolution of waves in magnetized regions and their coupling to radiative transfer is of major importance to a reliable measurement of Doppler signatures in spectral lines. This will greatly improve our ability to infer correctly the sub-surface structural and flow perturbations from the surface measurements of solar oscillations.

Acknowledgements This work has made use of the STOPRO routines within the SPINOR spectral inversion code developed by the 'Ground-based Solar Observations Group' at the Max-Planck Institute for Solar System Research, Katlenburg-Lindau, Germany. We especially thank Dr. Andreas Lagg for teaching us on the usage of SPINOR

code.

References

- N. Alamanni, F. Cavallini, G. Ceppatelli and A. Righini, *Astron. Astrophys.*, vol. 228, p. 517, 1990.
- H. Balthasar and W. Schmidt, *Astron. Astrophys.*, vol. 279, p. 243, 1993.
- T. J. Bogdan, *Solar Phys.*, vol. 192, p. 373, 2000.
- C. Frutiger, *Ph.D. Thesis*, Institute of Astronomy, ETH Zurich, No. 13896, 2000.
- S. S. Hasan, A. A. van Ballegooijen, W. Kalkofen and O. Steiner, *Astrophys. J.*, vol. 631, p. 1270, 2005.
- P. Maltby, E. H. Avrett, M. Carlsson, O. Kjeldseth-Moe, R. L. Kurucz and R. Loeser, *Astrophys. J.*, vol. 306, p. 284, 1986.
- P. H. Scherrer et al., *Solar Phys.*, vol. 162, p. 219, 1995.
- S. K. Solanki, *Ph.D. Thesis*, Institute of Astronomy, ETH Zurich, No. 8309, 1987.
- H. Uitenbroek, *Astrophys. J.*, vol. 592, p. 1225, 2003.
- W. Unno, Y. Osaki, H. Ando and H. Shibahashi, *Nonradial Oscillations of Stars*, 2nd ed., Tokyo: Univ. Tokyo Press, 1989.
- R. Wachter, *Ph.D. Thesis*, Institute of Astronomy, ETH Zurich, No.15514
- R. Wachter, J. Schou and K. Sankarasubrahmanian, *Astrophys. J.*, (submitted), 2006.